ARTICLE

Convenient Approach to γ-Fe_2O_3 Nanoparticles: Magnetic and Electrochemical Properties

Bei-bei Li[a], Ming-rong Ji[a*], Xiao-min Ni[b], Fu Zhou[b], Dong-en Zhang[b], Jing Cheng[b]

a. Hefei National Laboratory for Physical Sciences at Microscale, University of Science and Technology of China, Hefei 230026, China; b. Department of Chemistry, University of Science and Technology of China, Hefei 230026, China

(Dated: Received on April 17, 2006; Accepted on May 15, 2006)

A convenient approach is reported for the synthesis of spherical maghemite (γ-Fe_2O_3) nanoparticles. The process was realized by the controlled oxidation of Fe_3O_4 precursor, which originated from a facile partial-reduction co-precipitation process. The starting material of hydrosulfurous sodium ($Na_2S_2O_4$), which can allow reaction to proceed without any deoxygenated protection, was proven to be important in the formation of the precursor. A series of techniques, including X-ray diffraction, transmission electron microscopy and a vibrating sample magnetometer were used to characterize the product. The resultant γ-Fe_2O_3 nanoparticles exhibited ferromagnetism at 300 K and the values of saturation magnetization and coercivity were 70 emu/g and 164 Oe, respectively. The electrochemical properties of lithium ions intercalation into γ-Fe_2O_3 nanoparticles were tested in Teflon cells. A specific capacity of 933 mAh/g was delivered at a current density of 0.2 mA/cm^2 (voltage range 3.0-0.3 V *vs.* Li), corresponding to the reaction of 5.7 Li^+ per Fe_2O_3. A possible mechanism of the reaction of lithium with maghemite spinel was discussed.

Key words: Magnetic materials, Chemical synthesis, Electrochemical properties

I. INTRODUCTION

There has been an increasing interest in developing materials based on ferric oxides because of their potential application in many technological fields [1-5]. In particular, γ-Fe_2O_3 has been extensively investigated in view of their application in ferrofluids, bioprocessing, magnetic refrigeration, information storage, gas sensors and color imaging [6-11].

Nanomaterials with the size of 1-100 nm have been widely studied due to the departure of properties from bulk phases arising from quantum size effects. Therefore, much effort has been made to prepare γ-Fe_2O_3 nanoparticles, including co-precipitation, microemulsions, high temperature decomposition of organic precursors and the oxidation of magnetite [12-15]. Among them, the method of calcining Fe_3O_4 precursor in the air has been most applied, wherein Fe_3O_4 is commonly produced via co-precipitation of ferric (Fe^{3+}) and ferrous (Fe^{2+}) by a base, $NH_3{\cdot}H_2O$ or NaOH, in an aqueous solution [16-21]. However, procedures of this co-precipitation method are always complicated because a protective gas (usually nitrogen) must be bubbled with the solution to avoid oxidation of ferrous ions before precipitation. In this research, we simplify this tedious procedure by using hydrosulfurous sodium ($Na_2S_2O_4$) as a reductant. Fe_3O_4 nanoparticles were synthesized successfully without any deoxygenated protection. Then spherical maghemite (γ-Fe_2O_3) nanoparticles could be easily obtained by oxidizing as-prepared Fe_3O_4 precursor. Magnetic properties and electrochemical performances of the γ-Fe_2O_3 nanoparticles were investigated. The electrochemical tests were conducted at a current density of 0.2 mA/cm^2 (voltage range 3.0-0.3 V *vs.* Li) and the possible mechanism of the reaction of lithium with maghemite spinel was discussed.

II. EXPERIMENTS

A. Preparation of precursor of Fe_3O_4 and γ-Fe_2O_3

All the reagents used in the experiments were purchased from commercial sources and were used as received without further purification. A typical procedure for the synthesis of Fe_3O_4 was as follows: 0.13 g $Na_2S_2O_4$ was added to 3 mL $FeCl_3$ (1 mol/L) solution under slow magnetic stirring. Just after mixing, the color of the solution changed from light yellow to red, implying the formation of complex ions. When the color turned back to light yellow, 50 mL predetermined diluted $NH_3{\cdot}H_2O$ was poured into the solution quickly under vigorous stirring. A black precipitate formed at once, indicating the formation of Fe_3O_4. The stirring was continued for another 40 min to make the crystallization process complete. The precipitate was washed by magnetic decantation several times and then dried under vacuum at 40 °C for 12 h. Finally, the dried black magnetic powder was heated in an oven at air atmosphere at 300 °C for 12 h. The resultant red-brown powders were collected for characterization.

*Author to whom correspondence should be addressed. E-mail: jmr@ustc.edu.cn

B. Sample characterization

The crystalline phase of the products was investigated by XRD using a Philips X'Pert Pro Super diffractometer with Cu Kα radiation (λ=1.54178 Å) in the 2θ range of 10°-70°. Transmission electron microscopy (TEM) images were taken with a Hitachi model H-800 transmission electron microscope, using an acceleration voltage of 200 kV. The magnetic property was measured on a BHV-55 vibrating sample magnetometer at room temperature. The electrochemical properties of as-prepared samples were evaluated using a Teflon cell with a lithium metal anode. The cathode was a mixture of γ-Fe_2O_3/acetyleneblack/polyvinylidene fluoride (PVDF) with weight ratio of 80:10:10. The electrolyte was a 1 mol/L $LiPF_6$ in a 1:1 mixture of ethylene carbonate (EC)/diethyl carbonate (DEC) and the separator was Celgard 2500. The cells were assembled in a glove box filled with highly pure argon gas (O_2 and H_2O<5 μmol/L). The electrochemical tests were made in the voltage range of 3.0-0.3 V range at a current density of 0.2 mA/cm^2.

III. RESULTS AND DISCUSSION

XRD patterns of the as-prepared precursor γ-Fe_2O_3 are shown in Fig.1(a), in which all peaks can be assigned to the cubic-structured Fe_3O_4 (JCPDS 19-0629). The wide peaks indicate that precursor Fe_3O_4 with very small size has been obtained. Figure 1(b) exhibits the XRD patterns of final product. All the diffraction peaks can be readily indexed to a cubic spinel γ-Fe_2O_3 phase according to the literature values in JCPDS 39-1346.

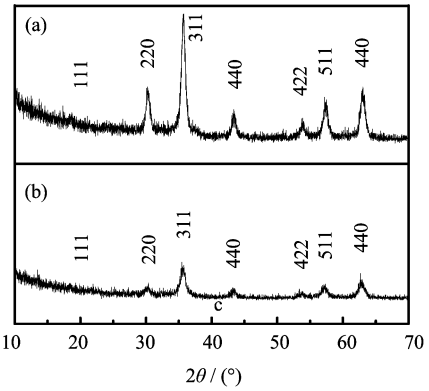

FIG. 1 XRD pattern of maghemite nanoparticles γ-Fe_2O_3 (a) and the as-prepared magnetite Fe_3O_4 (b).

Figure 2 shows the TEM images of the as-synthesized Fe_3O_4 and γ-Fe_2O_3, showing spherical-like shapes with average particle size of 10 and 13 nm, respectively. The insets are the corresponding selected area electron diffraction (SAED) pattern, revealing polycrystalline nature in both.

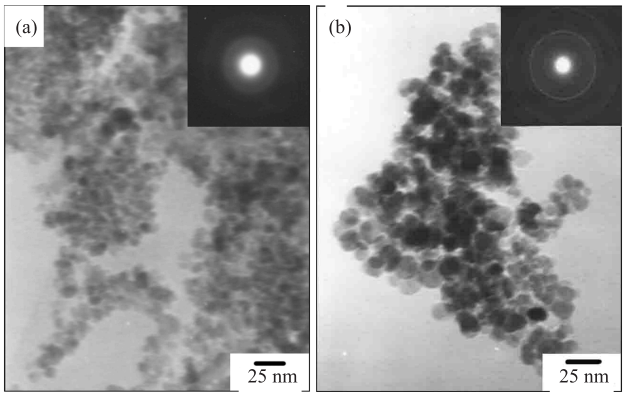

FIG. 2 TEM images and SAED (inset) patterns of Fe_3O_4 (a) and γ-Fe_2O_3 nanoparticles (b).

Commonly, formation of Fe_3O_4 by the co-precipitation of Fe^{3+} and Fe^{2+} must be processed under deoxygenated protection to prevent the oxidation of ferrous ions. As a result, protective gas (usually inert gases) must be bubbled into the solution, which always results in complicated equipment and complex procedures. In our experiment, we employ $Na_2S_2O_4$ as the reductant, which can allow the synthesis of Fe_3O_4 in air and greatly simplify the procedures. It is known that $Na_2S_2O_4$ is a strong reducing agent which can be easily oxidized by O_2. When added to the ferric solution, $Na_2S_2O_4$ serves as a deoxygenating agent, which consumes the oxygen dissolved in the water. Meanwhile, $SO_3{}^{2-}$ are generated, which can form a red complex with Fe^{3+} [22]. Subsequently, this unstable complex may transform into Fe^{2+} gradually, owing to the redox reaction between Fe^{3+} and $SO_3{}^{2-}$. Then small Fe_3O_4 particles are produced from the co-precipitation of Fe^{3+} and Fe^{2+} by adding dilute ammonia as soon as the color changes from red to yellow. The whole reaction could be expressed as:

$$S_2O_4{}^{2-} + 18Fe^{3+} + 56OH^- \rightarrow 2SO_4{}^{2-} + 6Fe_3O_4 \downarrow + 28H_2O \qquad (1)$$

If $Na_2S_2O_4$ is replaced by Na_2SO_3 or $Na_2S_2O_3$, keeping other conditions constant, only $Fe(OH)_3$ colloid is obtained in our system, proving the peculiar role of $Na_2S_2O_4$ for the preparation of Fe_3O_4 particles in air condition.

Figure 3 shows the magnetization-hysteresis (M-H) loop of the sample measured at 300 K, which indicates that the resultant γ-Fe_2O_3 nanoparticles exhibit ferromagnetism. The saturation magnetization (Ms) and coercivity (Hc) could be determined to be 70 emu/g and 164 Oe, respectively. Compared with those of the reported corresponding values (Hc=300 Oe and Ms=76 emu/g) for the much larger particles (average dimension=500 nm×10 nm) [23], these two values both decrease, possibly due to the superparamagnetism of some of the very small particles and the spherical mor-

ISSN 1003-7713/DOI:10.1360/cjcp2007.20(2).203.4

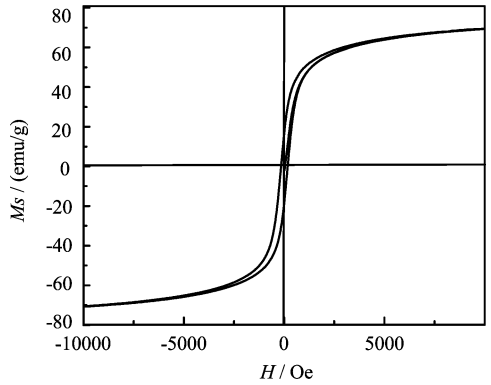

FIG. 3 M-H loop of the γ-Fe_2O_3 sample.

phology with low shape anisotropy [24,25].

Electrochemical tests were conducted to investigate the electrochemical performance of the as-prepared sample in the cell configuration of γ-Fe_2O_3/Li. Figure 4 illustrates potential *vs.* capacity curve for the first discharge carried out in a galvanostatic mode at 0.2 mA/cm^2 in the voltage range 3.0-0.3 V (*vs.* Li). The initial discharge capacity of the γ-Fe_2O_3 nanoparticles in the intercalation-deintercalation cycle of Li^+ can reach 933 mAh/g (lithium capacity up to 5.7 Li/Fe). Such a high first discharge capacity may be attributed to the larger surface or interface arising from the small particle size, which facilitates the intercalation-deintercalation of lithium ions [26].

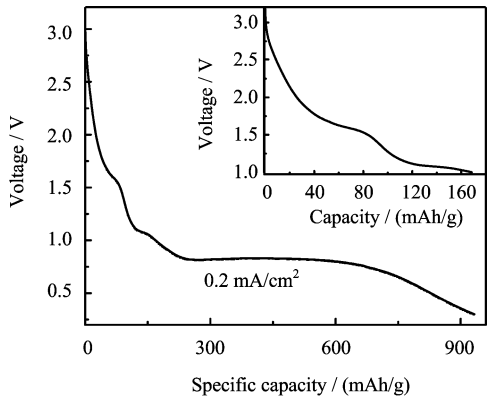

FIG. 4 Discharge curve for the obtained maghemite sample in a voltage window of 3.0-0.3 V. Inset: Part of the discharge curve in a voltage window of 3.0-1.0 V.

The mechanism of the reaction of lithium with maghemite spinel might be as follows. The electrochemical Li insertion into the maghemite, which has a defective spinel structure written as $[Fe^{3+}]_{8a}[Fe^{3+}{}_{5/3}Fe^{2+}{}_{1/3}]_{16d}O_4$ in spinel notation [27], begins with the filling of the octahedral vacancies. Then the voltage drops slowly between 1.6-1.0 V (as seen in the inset of Fig.4). In this region, the lithium insertion reaction involves two successive steps: (i) a spinel to rocksalt transition reaction which consists of a major rearrangement of the structure including the cooperative motion of 8a tetrahedral Fe^{3+} towards the 16c octahedral sites; (ii) occupation of the rest of the 16c sites with the increasing insertion of Li^+ [27]. As the lithium insertion precedes, a distinctive plateau of 0.84 V can be observed, which corresponds to the reduction of Fe(III)-Fe(0) [28,29]. The whole processes can be described as follows:

$$Fe_2O_3+6Li \underset{\text{Charge}}{\overset{\text{Discharge}}{\Longleftrightarrow}} 2Fe + 3Li_2O \qquad (2)$$

IV. CONCLUSION

In summary, spherical maghemite (γ-Fe_2O_3) nanoparticles with an average diameter of 13 nm have been prepared via a convenient way. The process was realized by the oxidation of Fe_3O_4 precursor, which originated from a facile partial-reduction co-precipitation process. The starting material of hydrosulfurous sodium ($Na_2S_2O_4$), which allows the reaction without the need for any deoxygenated protection, was proved important in the formation of the precursor. The products were investigated by XRD, TEM and VSM. The resultant γ-Fe_2O_3 nanoparticles exhibited ferromagnetism at 300 K and the values of saturation magnetization (Ms) and coercivity (Hc) were 70 emu/g and 164 Oe, respectively. The electrochemical properties of lithium ions intercalation into γ-Fe_2O_3 nanoparticles were tested in Teflon cells. The product delivered a specific capacity of 933 mAh/g at a current density of 0.2 mA/cm^2 (voltage range 3.0-0.3 V *vs.* Li), corresponding to the reaction of 5.7 Li^+ per Fe_2O_3. A possible mechanism of the reaction of lithium with maghemite spinel was discussed.

V. ACKNOWLEDGMENTS

The authors are grateful for the financial support from the State Key Lab of Fire Science (HZ2005-KF11) and the electrochemical characterization assistance from Highstar Chemical Powder Source Company Limited.

[1] G. P. Vissokov and P. S. Pirgov, J. Mater. Sci. **31**, 4007 (1996).
[2] C. R. Catlow, J. Corish, J. Hennesy and W. C. Mackrodt, J. Am. Ceram. Soc. **71**, 42 (1988).
[3] Y. Nakatani, M. Sakai and M. Matsuoka, Jpn. J. Appl. Phys. 22, 912 (1983).
[4] R. F. Ziolo, E. P. Giannelis, B. A. Weinstein, M. P. O'Horo, B. N. Ganguly, V. Mehrothra, *et al.* Science **257**, 219 (1992).

ISSN 1003-7713/DOI:10.1360/cjcp2007.20(2).203.4

[5] J. K. Vassiliou, V. Mehrothra, M. W. Russell and E. P. Giannelis, J. Appl. Phys. **73**, 5109 (1993).
[6] I. J. Anton, Magn. Magn. Mater. **85**, 219 (1990).
[7] W. Chang, M. Deng, T. Tsai and T. Ching, Jpn. J. Appl. Phys. **31**, 1343 (1992).
[8] T. Gonzalez-Carreno, A. Mifsud, J. M. Palacios and C. J. Serna, Mater. Chem. Phys. **27**, 287 (1991).
[9] V. Chhabra, P. Ayyub, S. Chattopadhyay and A. N. Maitra. Mater. Lett. **26**, 21 (1996).
[10] K. Suresh and K. C. Patil, J. Mater. Sci. Lett. **12**, 572 (1993).
[11] L. Nixon, C. A. Koval and R. D. Noble, Chem. Mater. **4**, 117 (1992).
[12] J. Lee, T. Isobe and M. Senna, J. Colloid Interface Sci. **177**, 490 (1996).
[13] N. Feltin and M. P. Pileni, Langmiur **13**, 3927 (1997).
[14] H. Hyeon, S. S. Lee, J. Park, Y. Chung and H. B. Na, J. Am. Chem. Soc. **123**, 12798 (2001).
[15] Y. S. Kang, S. Risbud, J. P. Tabolt and P. Stroeve, Chem. Matter. **8**, 2209 (1996).
[16] Z. H. Zhou, J. Wang, X. Liu and H. S. O. Chan, J. Mater. Chem. **11**, 1704 (2001).
[17] J. Wang, Q. W. Chan, C. Zeng and B. Y. Hou, Adv. Mater. **16**, 137 (2004).
[18] Y. H. Ni, X. W. Ge, Z. C. Zhang and Q. Ye, Chem. Mater. **14**, 1048 (2002).
[19] T. Fried, G. Shemer and G. Markovich, Adv. Mater. **13**, 1158 (2001).
[20] Y. Sahoo, M. Cheon, S. Wang, H. Luo, E. P. Furlani and P. N. Prasad, J. Phys. Chem. B **108**, 3380 (2004).
[21] J. Wang, J. J. Sun, Q. Sun and Q. W. Chen, Mater. Res. Bull. **38**, 1113 (2003).
[22] E. Danilczuk and A. Swinarski, Roczn. Chem. **35**, 1563 (1961).
[23] J. C. Mallinson, *The Foundations of Magnetic Recording, 2nd edn.*, San Diego: Academic Press, 29 (1993).
[24] J. M. D. Coey, Phys. Rev. Lett. **27**, 1140 (1971).
[25] D. L. Leslie-Pelecky and R. D. Rieke, Chem. Mater. **8**, 1770 (1996).
[26] X. Wang, X. Y. Chen, L. S. Gao, H. G. Zheng and Z. D. Zhang, J. Phys. Chem. B **108**, 16401 (2004).
[27] M. Pernet, P. Strobel, B. Bonnet, P. Bordet and Y. Chabre, Solid State Ionics **66**, 259 (1993).
[28] X. H. Yang , X. Wang and Z. D. Zhang, J. Crystal Growth **277**, 467 (2005).
[29] X. Wang, L. S. Gao, H. G . Zheng, M. R. Ji, T. Shen and Z. D. Zhang, J. Crystal Growth **269**, 489 (2004).

ISSN 1003-7713/DOI:10.1360/cjcp2007.20(2).203.4